Behavioral/Cognitive

Growth Hormone Action in Somatostatin Neurons Regulates Anxiety and Fear Memory

Willian O. dos Santos,[1] Vitor A. L. Juliano,[2] Fernanda M. Chaves,[1] Henrique R. Vieira,[3] Renata Frazao,[3] Edward O. List,[4] John J. Kopchick,[4] Carolina D. Munhoz,[2] and Jose Donato Jr[1]

[1]Department of Physiology and Biophysics, Instituto de Ciencias Biomedicas, Universidade de São Paulo, São Paulo 05508-000, Brazil, [2]Department of Pharmacology, Instituto de Ciencias Biomedicas, Universidade de São Paulo, São Paulo 05508-000, Brazil, [3]Department of Anatomy, Instituto de Ciencias Biomedicas, Universidade de São Paulo, São Paulo 05508-900, Brazil, and [4]Edison Biotechnology Institute and Heritage College of Osteopathic Medicine, Ohio University, Athens 45701, Ohio

Dysfunctions in growth hormone (GH) secretion increase the prevalence of anxiety and other neuropsychiatric diseases. GH receptor (GHR) signaling in the amygdala has been associated with fear memory, a key feature of posttraumatic stress disorder. However, it is currently unknown which neuronal population is targeted by GH action to influence the development of neuropsychiatric diseases. Here, we showed that approximately 60% of somatostatin (SST)-expressing neurons in the extended amygdala are directly responsive to GH. GHR ablation in SST-expressing cells ($SST^{\Delta GHR}$ mice) caused no alterations in energy or glucose metabolism. Notably, $SST^{\Delta GHR}$ male mice exhibited increased anxiety-like behavior in the light-dark box and elevated plus maze tests, whereas $SST^{\Delta GHR}$ females showed no changes in anxiety. Using auditory Pavlovian fear conditioning, both male and female $SST^{\Delta GHR}$ mice exhibited a significant reduction in fear memory. Conversely, GHR ablation in SST neurons did not affect memory in the novel object recognition test. Gene expression was analyzed in a micro punch comprising the central nucleus of the amygdala (CEA) and basolateral (BLA) complex. GHR ablation in SST neurons caused sex-dependent changes in the expression of factors involved in synaptic plasticity and function. In conclusion, GHR expression in SST neurons is necessary to regulate anxiety in males, but not female mice. GHR ablation in SST neurons also decreases fear memory and affects gene expression in the amygdala, although marked sex differences were observed. Our findings identified for the first time a neurochemically-defined neuronal population responsible for mediating the effects of GH on behavioral aspects associated with neuropsychiatric diseases.

Key words: **amygdala; anxiety; fear memory; GH; neuropsychiatric disorders; somatostatin**

Significance Statement

Hormone action in the brain regulates different neurological aspects, affecting the predisposition to neuropsychiatric disorders, like depression, anxiety, and posttraumatic stress disorder. Growth hormone (GH) receptor is widely expressed in the brain, but the exact function of neuronal GH action is not fully understood. Here, we showed that mice lacking the GH receptor in a group of neurons that express the neuropeptide somatostatin exhibit increased anxiety. However, this effect is only observed in male mice. In contrast, the absence of the GH receptor in somatostatin-expressing neurons decreases fear memory, a key feature of posttraumatic stress disorder, in males and females. Thus, our study identified a specific group of neurons in which GH acts to affect the predisposition to neuropsychiatric diseases.

Received Feb. 10, 2023; revised July 28, 2023; accepted Aug. 20, 2023.

Author contributions: J.D. designed research; W.O.d.S., V.A.L.J., F.M.C., H.R.V., and R.F. performed research; R.F., E.O.L., and J.J.K. contributed unpublished reagents/analytic tools; W.O.d.S., V.A.L.J., F.M.C., H.R.V., C.D.M., and J.D. analyzed data; V.A.L.J., R.F., E.O.L., J.J.K., and C.D.M. edited the paper; J.D. wrote the paper.

This work was supported by Fundação de Amparo à Pesquisa do Estado de São Paulo FAPESP)/Brazil Grants 2017/21854-9 (to F.M.C.), 2019/21707-1 (to R.F.), and 2020/01318-8 (to J.D.); the National Institutes of Health National Institute on Aging Grant R01AG059779 (to J.J.K. and E.O.L.); the Coordenação de Aperfeiçoamento de Pessoal de Nível Superior (CAPES)/Brazil Finance Code 001 (to W.O.d.S. and H.R.V.); and the Conselho Nacional de Desenvolvimento Científico e Tecnológico (CNPq)/Brazil Grant 303363/2019-3 (to J.D.). We thank Ana M. P. Campos for her technical assistance.

The authors declare no competing financial interests.

Correspondence should be addressed to Jose Donato Jr at jdonato@icb.usp.br.

https://doi.org/10.1523/JNEUROSCI.0254-23.2023

Introduction

Millions of people suffer from neuropsychiatric diseases, including depression, anxiety, and posttraumatic stress disorder, causing numerous impairments to these individuals. Growing evidence suggests that hormones may play a role in regulating different neurological aspects, altering the predisposition to these disorders. For example, changes in sex hormone levels, particularly estradiol, affect anxiety-like or depression-like behavior and fear memory in rodents and humans (Walf et al., 2009; Walf and Frye, 2010; Zeidan et al., 2011). Other studies have shown that glucocorticoids may be involved in the pathogenesis of neuropsychiatric diseases (Binder, 2009; Claes, 2009; Chiba et al., 2012).

There is evidence that children and adults with growth hormone (GH) deficiency present a higher prevalence of anxiety and depression (Karachaliou et al., 2021). However, it is still unknown how GH can affect the prevalence of neuropsychiatric diseases. In the last years, our group has shown that several brain structures associated with neuropsychiatric disorders contain a large number of neurons directly responsive to GH (Furigo et al., 2017; Wasinski et al., 2021a). These GH-responsive areas include the hypothalamus, hippocampus, amygdala, bed nucleus of the stria terminalis (BNST), and some brainstem nuclei. A previous study showed that approximately two-thirds of corticotropin-releasing hormone (CRH)-expressing neurons in the mouse paraventricular nucleus of the hypothalamus (PVH) exhibit phosphorylation of the signal transducer and activator of transcription 5 (pSTAT5) after a systemic GH injection, which indicates activation of GH receptor (GHR) and its downstream intracellular pathway (Quaresma et al., 2021). Since PVH^{CRH} neurons are important regulators of the stress response, GH action on this neuronal population may be associated with neuropsychiatric disorders. However, GHR ablation in CRH-expressing cells causes no behavioral alteration in mice (Dos Santos et al., 2021).

GH-responsive cells are largely found in the extended amygdala, particularly in the central nucleus of the amygdala (CEA) and dorsolateral BNST (Furigo et al., 2017; Wasinski et al., 2021a). These nuclei contain several neurochemically-defined neuronal populations, including cells that express CRH, protein kinase Cδ, somatostatin (SST), and tachykinin 2 (Ye and Veinante, 2019). Inhibition of CEA^{CRH} neurons causes anxiolytic effects via projections to the dorsolateral BNST (Pomrenze et al., 2019). Although part of CEA^{CRH} and $BNST^{CRH}$ neurons is responsive to GH, CRH-specific GHR knock-out mice exhibit normal anxiety and stress response (Dos Santos et al., 2021). In addition to pituitary-derived GH, previous studies have suggested that basolateral amygdala (BLA) may locally produce GH. Chronic stress not only increases fear memory but also the expression of GH in the BLA (Meyer et al., 2014). Virus-mediated GH overexpression in the BLA increases the number of cells activated by fear memory formation and dendritic spine density in the amygdala (Gisabella et al., 2016). Thus, amygdala neurons may be affected by either pituitary-derived or locally-derived GH. However, no information exists about the neuronal population in the amygdala that expresses the GHR to regulate fear responses.

SST-expressing neurons are involved in several functions, including the control of GH secretion (Steyn et al., 2016), food intake (Luo et al., 2018; Stengel and Taché, 2019; Kumar and Singh, 2020) and anxiety (Engin et al., 2008; Engin and Treit, 2009; Wohleb et al., 2016; Fuchs et al., 2017). While hypothalamic SST neurons regulate the somatotropic axis and metabolism, SST neurons in the extended amygdala are associated with changes in anxiety (Pantazopoulos et al., 2017; Ahrens et al., 2018; Sun et al., 2020; Bruzsik et al., 2021; Xiao et al., 2021) and fear memory (H. Li et al., 2013; Penzo et al., 2015; Besnard et al., 2019; Sun et al., 2020; Bruzsik et al., 2021). Whether SST neurons in the extended amygdala are responsive to GH, and SST-expressing cells mediate the effects of GH regulating anxiety and fear memory is still unknown. To understand how central GHR signaling can alter the predisposition to neuropsychiatric diseases, our study aims to determine whether GHR expression in SST neurons is necessary to regulate anxiety and fear memory in male and female mice.

Materials and Methods

Mice

To visualize SST-expressing cells, the SST^{Cre} mouse model (The Jackson Laboratory; RRID: IMSR_JAX:018973) was crossed with mice expressing a Cre-dependent enhanced green fluorescent protein (eGFP; The Jackson Laboratory; RRID: IMSR_JAX:026175). GHR ablation specifically in SST-expressing cells was achieved by breeding the SST^{Cre} mice with animals carrying loxP-flanked *Ghr* alleles (List et al., 2013). The experiments used only $Ghr^{flox/flox}$ mice and the control group was composed of littermates negative for the Cre allele, whereas $SST^{\Delta GHR}$ mice carried the SST^{Cre} gene in heterozygosity. Mice were in the C57BL/6J background and were produced and maintained in standard conditions of light (12/12 h light/dark cycle; lights on at 8 A.M.) with *ad libitum* access to regular rodent chow and filtered water. The experimental procedures were approved by the Ethics Committee on the Use of Animals of the Instituto de Ciencias Biomedicas at the Universidade de São Paulo.

Identification of GH-responsive and estrogen-responsive neurons

Adult SST-eGFP reporter male and female mice (n = 3–5/group) received an intraperitoneal injection of saline or GH (20 μg/g) extracted from porcine pituitary (National Hormone and Pituitary Program, Torrance, CA) and were perfused 90 min later. Mice were anesthetized with isoflurane and perfused transcardially with saline, followed by a 10% buffered formalin solution. Brains were collected and postfixed in the same fixative for 45 min and cryoprotected overnight at 4°C in 0.1 M PBS containing 20% sucrose. Brains were cut into 30-μm-thick sections using a freezing microtome. Brain slices were rinsed in 0.02 M potassium PBS, pH 7.4 (KPBS), followed by pretreatment in a water solution containing 1% hydrogen peroxide and 1% sodium hydroxide for 20 min. After rinsing in KPBS, sections were incubated in 0.3% glycine and 0.03% lauryl sulfate for 10 min each. Next, slices were blocked in 3% normal serum for 1 h, followed by incubation in a primary antibody cocktail containing anti-$phospho^{Tyr694}$-STAT5 (1:1000; Cell Signaling Technology; catalog #9351; RRID: AB_2315225) and anti-eGFP (1:5000; Aves Labs; catalog #GFP-1020; RRID: AB_10000240) for 40 h. Subsequently, sections were rinsed in KPBS and incubated for 90 min in Alexa Fluor-conjugated secondary antibodies (1:500, Jackson ImmunoResearch Laboratories). After rinsing in KPBS, sections were mounted onto gelatin-coated slides and covered with Fluoromount G mounting medium (Electron Microscopic Sciences). The colocalization between estrogen receptor α (ERα) and eGFP (SST neurons) was performed as described above, except that we used the primary antibody anti-ERα (1:20,000, MilliporeSigma; catalog #04-1564; RRID: AB_10618636). A Zeiss Axiocam 512 color camera adapted to an Axioimager A1 microscope (Zeiss) was used to obtain the photomicrographs. Single-labeled and double-labeled cells were manually counted using the counting tool available in the Adobe Photoshop software.

Evaluation of energy and glucose homeostasis

Body weight and body composition were analyzed in approximately five-month-old male and female mice using time-domain nuclear magnetic resonance (LF50 body composition mice analyzer; Bruker). Subsequently, mice were single-housed for acclimation. Then, food intake was measured by recording the amount of daily food ingested for 5 consecutive days. O_2 consumption (VO_2), CO_2 production, respiratory quotient (CO_2 production/O_2 consumption), and ambulatory activity (by infrared sensors) were analyzed by the Oxymax/Comprehensive Lab Animal Monitoring System (Columbus Instruments) for approximately 7 d. The data from the first 2 d of analysis were discarded because we considered the acclimatization period. The results used for each animal were the average of the analyzed days. In the experiments that evaluated glucose homeostasis, food was removed from the cage 4 h before each test, and after determining basal glucose levels (time 0), mice received intraperitoneal injections of 2 g/kg of glucose, 1 IU/kg of insulin or 0.5 g/kg of 2-deoxy-D-glucose (2DG; MilliporeSigma), followed by serial determinations of blood glucose levels using a glucose meter through samples collected from the tail tip. The area under the curve of blood glucose levels was calculated for each test per animal using the Prism software version 8.4.3 (GraphPad).

Anxiety tests

Another group of mice was evaluated in the behavioral experiments. In the open field test, adult mice were placed in an arena [40 cm (w) × 40 cm (d) × 30 cm (h)] and their behavioral states were evaluated for 5 min. In this regard, total distance traveled, time spent and number of entries in the center of the arena, and duration and frequency of grooming, walking, rearing, sniffing, and stationary state were determined. The light-dark box test used a box divided into two compartments (light and dark), where each compartment measures 21.5 × 40.5 × 21 cm and with an open central access (5 × 5 cm) between them, positioned on a flat surface. The light compartment was entirely white, except for the translucent lid, with a luminosity of 400-lx considered aversive, and the dark compartment, entirely black, with a luminosity of 3 lx. All animals were placed individually at the end of the white compartment with their muzzle facing the central access, with complete freedom to explore the entire box for 5 min. The following parameters were analyzed: time spent in the light compartment, number of crossings between the compartments and distance traveled in the light zone. After each behavioral test, the boxes were cleaned with 5% alcohol to avoid olfactory cues. In the elevated plus maze test, we used an apparatus that is elevated 40 cm from the ground and it is composed of two opposite open arms measuring 35 × 5 cm, crossed by two closed arms of similar dimensions. Each animal was placed in the center of the apparatus and the number of entries, the distance traveled, and the time spent in the open arms were measured for 5 min. The animal's position and movements were recorded and analyzed by the ANY-maze software (Stoelting Co.). After each test, the apparatuses were cleaned with 70% ethanol and air-dried before a new trial.

Auditory Pavlovian fear conditioning

This test initially used a conditioning box (28 × 26 × 23 cm) consisting of four white walls, a transparent acrylic lid, and a base formed by metallic bars that conduct electric current arranged in parallel (diameter of 0.4 cm and spacing between them of 1.05 cm) and connected to an electric shock generator (Insight Equipamentos). For the fear conditioning procedure, the mice were placed in the conditioning chamber for 2 min to habituate. After that, they were presented to three tone-shock pairings, consisting in tones of 3 kHz, 80 dB, 30 s each (conditioned stimulus, CS) paired with foot shocks (unconditioned stimulus, US: 0.6 mA, presented in the last 2 s of each sound). The intertrial interval was 60 s. Two minutes after the last CS-US pairing, the animals returned to their respective housing boxes. Between each session, the box was cleaned with a 79.5% water/19.5% alcohol/1% vanilla essence solution (Dr. Oetker). After 24 h, the fear of the tone was tested in a novel context consisting of a box measuring 22.5 × 19.5 × 27 cm, with a conical wall and floor covered with white self-adhesive paper. The session consisted of 2 min of habituation (Pre), followed by 40 CS presentations with a duration of 30 s each and 5-s intervals between them, in the absence of the US. The percentage of time in freezing was displayed in 200-s intervals. The mean percentage in freezing was also calculated for each animal.

Recognition memory

For the novel object recognition test, mice were acclimatized in the arena used in the open field for 5 min. On the next day, the training session consisted of a 5-min-long session in which the mice were placed at the bottom of the arena with their back to the two identical objects, and the time spent exploring each object was recorded. Approximately 24 h after the training session, animals were reinserted into the arena and one of the two objects used in the training session was replaced by a new one with a similar size. The time exploring the new and old objects was measured. During behavioral sessions, objects were fixed with tape to the floor so that the animals could not move them and none of the objects used evoked innate preference. The arena and stimulus objects were cleaned thoroughly between trials with 70% ethanol. The results are expressed as the percentage of time exploring each object during the training or test session in relation to total exploration time.

Quantitative real-time PCR

Control and $SST^{\Delta GHR}$ male and female mice were anesthetized with isoflurane, euthanized by decapitation, and the entire brain was removed. A coronal brain section (600 μm) was cut with a vibratome. A bilateral micro punch comprising the CEA and BLA (bregma: −1.06 to −1.66 mm) were collected using an 18-gauge needle and stored at −80°C. Total RNA from the bilateral micro punch was extracted using the Arcturus PicoPure RNA Isolation kit (Thermo Fisher Scientific; catalog #KIT0204; RID: SCR_008817), following the manufacturer's instructions. Assessment of RNA quantity and quality was performed with an Epoch Microplate Spectrophotometer (BioTek; RRID: SCR_017317). cDNA was synthesized by reverse transcription using 500 ng of RNA, SuperScript II Reverse Transcriptase (Invitrogen), and random primers p(dN)6 (MilliporeSigma). Quantitative real-time PCR was performed using the 7500TM Real-Time PCR System (Applied Biosystems), SYBR Green Gene Expression PCR Master Mix (Applied Biosystems), and specific primers for target genes (Table 1). Data were normalized to the geometric average of *Actb* and *Ppia* and reported as fold changes compared to values obtained from the control group (set at 1.0). Relative quantification of mRNA was calculated by $2^{-\Delta\Delta Ct}$.

Table 1. Primer sequences

Target gene	Forward primer	Reverse primer
Actb	gctccggcatgtgcaaag	catcacaccctggtgccta
Bdnf	atgttccaccaggtgagaag	gccttcatgcaaccgaagta
Creb1	actcagccgggtactaccat	cctgaggcagcttgaacaac
Crh	caacctcagccggttctgat	ggaaaaagttagccgcagcc
Dlg4	agttgcaggtgaacggaaca	cccagacctgagttacccctt
Dr2d	agtttcccagtgaacaggcg	ggctataccgggtcctctct
Gabbr1	tcccggagcatctgtagtca	atactgcacgccgttctgag
Gabbr2	agtcacgggtcaagttgtgtt	gttgtactcgccgaccttca
Gabra1	agcacactgtcgggaagaag	gtccagcagtcggtccaaaa
Gh	catgcccttgtccagtctgt	gtaggcacgctcgaactctt
Ghr	atcaatccaagcctggggac	acagctgaatagatcctgggg
Ghsr	ctcagggaccagaaccacaa	agccagcagaggatgaaagc
Gria1	cggaagtaaggacaagaccagt	ccaatcccagccctccaatc
Grin1	cgtgaacgtgtggaggaaga	cccggtgctcgtgtcttt
Grin2a	aattgctctgcagaagggctc	ccatctcaccgtcaccaacaa
Grin2b	ttacaaccggtgcctagctg	accaaatcgctttgccgatg
Kcnj8	catggagaagagtggcctgg	cgcagacgtgaatgacctga
Kcnj11	gctgtcccgaaagggcatta	cctcctctctcgagtacggt
Nrg1	gaggtgagaacacccaagtca	cagtcgtggatgtagatgtgg
Ppia	tatctgcactgccaagactgagt	cttcttgctggtcttgccattcc
Slc17a7	gtcacatacctgcttgcca	cccagcataggaaccgcaa
Slc32a1	gggtcacgacaaacccaaga	gcacgaacatgccctgaatg
Sst	ctgtcctgccgtctccagt	ctgcagaaactgacggagtct
Syp	gcagtgggtctttgccatct	actctccgtcttgttggcac

Statistical analysis

The differences between groups were analyzed by the unpaired two-tailed Student's *t* test. Two-way ANOVA was used to analyze the histological data. Freezing behavior over time and the percentage of exploration of different objects were analyzed by repeated measures two-way ANOVA. Statistical analyses were performed using the Prism software. All results were expressed as mean ± SEM, and only p values <0.05 were considered to be statistically significant.

Results

Distribution of SST-expressing neurons that are responsive to GH in the mouse brain

Several brain nuclei contain SST-expressing neurons, including the dorsolateral BNST, PVH, periventricular nucleus (PV), arcuate nucleus of the hypothalamus (ARH), tuberal nucleus (TU), and lateral CEA (Fig. 1). To identify specific neuronal populations that express functional GHR, we used the ability of a systemic GH injection to induce the activation of the GHR/STAT5 pathway, as previously shown (Furigo et al., 2017; Wasinski et al., 2021a). SST-eGFP reporter mice that received an intraperitoneal saline injection before the perfusion exhibited a small amount of

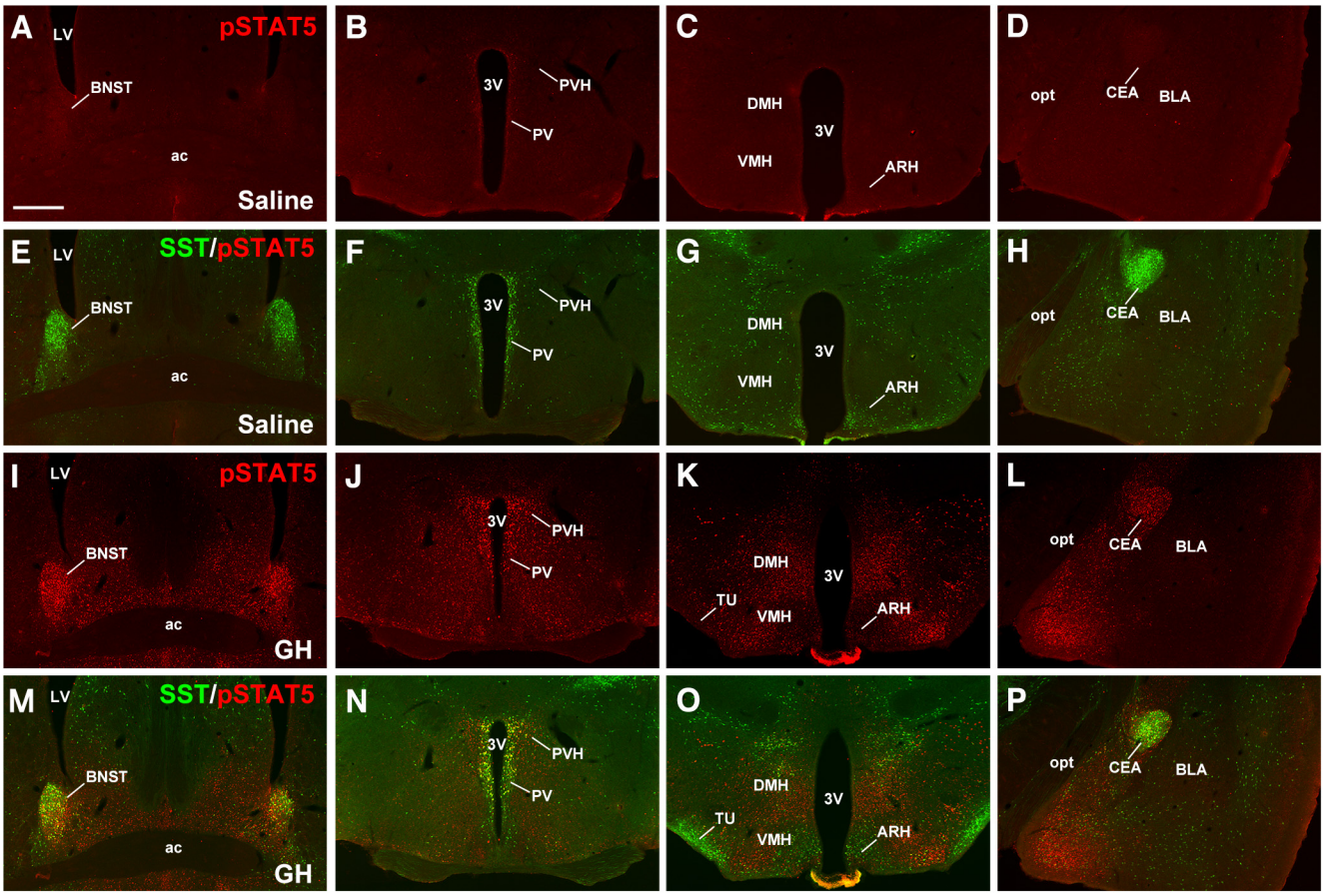

Figure 1. SST neurons of different brain nuclei are responsive to GH. ***A–H***, Epifluorescence photomicrographs showing pSTAT5 (red) and eGFP (green representing SST-expressing cells) immunoreactive neurons in the brain of an SST-eGFP reporter mouse that received an intraperitoneal injection of saline. ***I–P***, Photomicrographs showing pSTAT5 and eGFP immunoreactive neurons in the brain of an SST-eGFP reporter mouse that received an intraperitoneal injection of GH (20 μg/g b.w.) and was perfused 90 min later. Double-labeled neurons may appear as yellow. 3V, third ventricle; ac, anterior commissure; ARH, arcuate nucleus of the hypothalamus; BLA, basolateral amygdala; BNST, bed nucleus of the stria terminalis; CEA, central nucleus of the amygdala; DMH, dorsomedial nucleus of the hypothalamus; LV, lateral ventricle; opt, optic tract; PV, periventricular nucleus, PVH, paraventricular nucleus of the hypothalamus; TU, tuberal nucleus; VMH, ventromedial nucleus. Scale bar = 500 μm.

pSTAT5 immunoreactive cells in the mouse brain and very few co-localizations with SST-expressing neurons (Fig. 1*A–H*). In contrast, an intraperitoneal GH injection induced a robust pSTAT5 expression in several brain nuclei (Fig. 1*I–L*). Importantly, numerous co-localizations between GH-induced pSTAT5 and SST were observed in the BNST (Fig. 1*M*), PVH (Fig. 1*N*), PV (Fig. 1*N*), and CEA (Fig. 1*P*). Several GH-responsive SST neurons were also observed in the ARH (Fig. 1*O*) but just a few co-localizations were observed in the TU (Fig. 1*O*).

A previous study has shown that approximately 60% of PVH^{SST} and PV^{SST} neurons express pSTAT5 after a systemic GH injection (Chaves et al., 2022). In the current study, we quantify this co-expression in other brain nuclei of control male and female mice. We observed that approximately 20% of ARH^{SST} neurons contained GH-induced pSTAT5 (Fig. 2*A*). Notably, 62% and 60% of $BNST^{SST}$ (Fig. 2*B*) and CEA^{SST} neurons (Fig. 2*C*), respectively, were responsive to GH using a SST-eGFP reporter mouse model. The percentage of SST neurons that were responsive to GH was similar between males and females (Fig. 2*G–I*). Furthermore, male and female mice exhibited similar numbers of ARH^{SST}, $BNST^{SST}$, and CEA^{SST} neurons (Fig. 2*J–L*). To determine the physiological importance of GHR signaling in SST neurons, mice carrying inactivation of the *Ghr* gene exclusively in SST-expressing cells were produced ($SST^{\Delta GHR}$ mice). In contrast to the results observed in control animals, $SST^{\Delta GHR}$ mice exhibited few SST neurons containing GH-induced pSTAT5 in the ARH (Fig. 2*D*,*G*), BNST (Fig. 2*E*,*H*) and CEA (Fig. 2*F*,*I*). Moreover, pSTAT5 expression was intact in cells surrounding the SST neurons of $SST^{\Delta GHR}$ mice. Thus, these findings validate the efficacy and specificity of the GHR ablation only in SST-expressing cells. Interestingly, $SST^{\Delta GHR}$ male mice showed a reduced number of ARH^{SST} neurons, compared to control males, whereas the number of ARH^{SST} neurons was similar between control and $SST^{\Delta GHR}$ females (Fig. 2*J*). GHR ablation in SST-expressing cells did not affect the number of SST neurons in the BNST and CEA (Fig. 2*K*,*L*).

GHR ablation in SST neurons does not affect energy and glucose metabolism

Several studies revealed that SST neurons of different brain areas regulate food intake and other metabolic aspects (Campbell et al., 2017; Zhu et al., 2017; Luo et al., 2018; Zséli et al., 2018; Stengel and Taché, 2019; Kumar and Singh, 2020; Suresh Nair et al., 2022). Central GH action also modulates metabolism and stimulates feeding in different species, such as fish, rodents, and humans (Nyberg, 2000; Bohlooly-Y et al., 2005; Egecioglu et al., 2006; Deepak et al., 2008; Zhong et al., 2013; Kim et al., 2015; Furigo et al., 2019a, b; Quaresma et al., 2019; Teixeira et al., 2019; Donato et al., 2021; Gupta et al., 2021; Wasinski et al., 2021b; Stilgenbauer et al., 2023; Tavares et al., 2023). Thus, SST

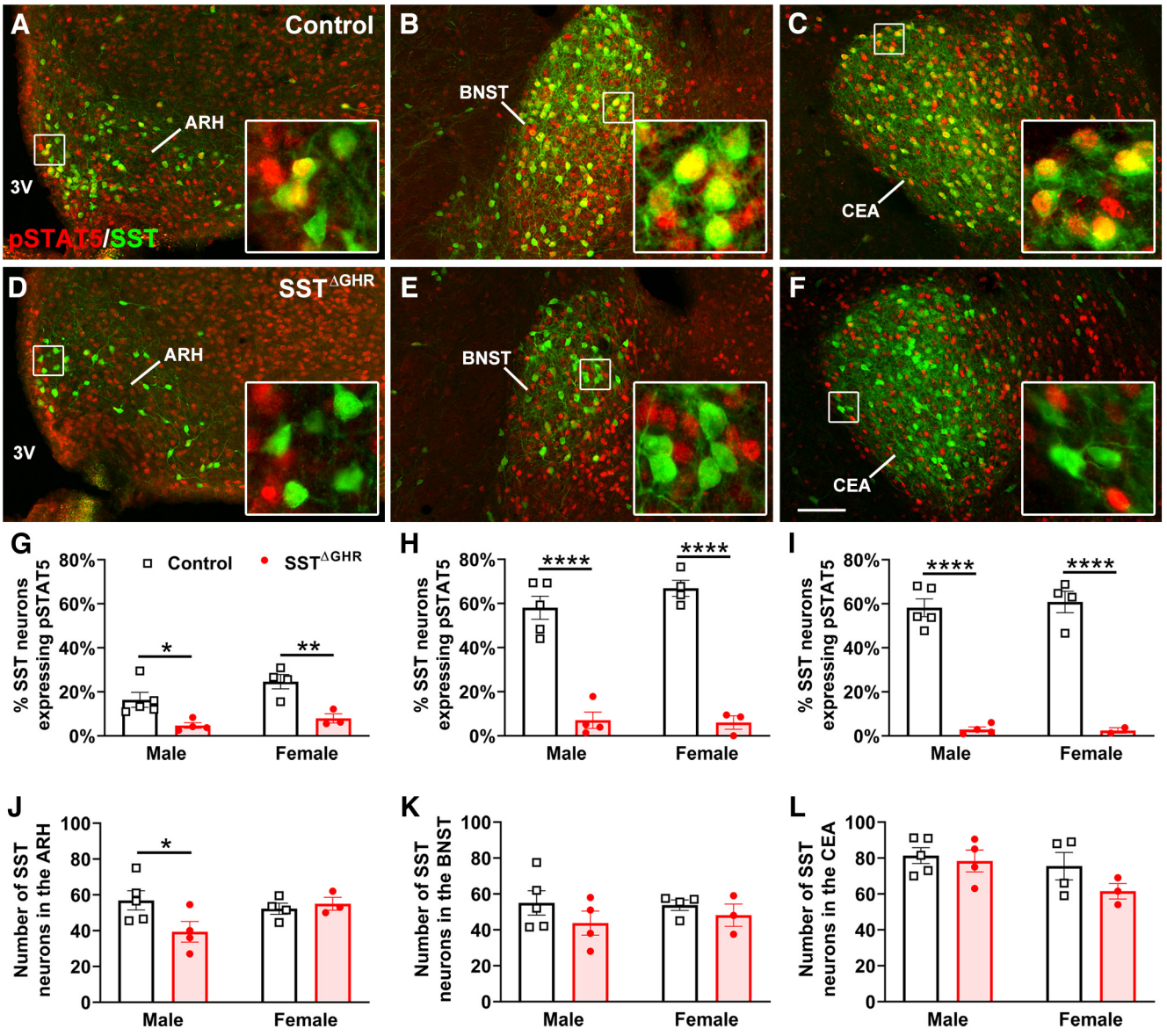

Figure 2. Validation of mice carrying GHR ablation specifically in SST-expressing cells. ***A–C***, Epifluorescence photomicrographs showing the co-localization between pSTAT5 (red) and eGFP (green representing SST-expressing cells) in SST-eGFP reporter control mice that received an intraperitoneal injection of GH before perfusion. The insets represent higher magnification photomicrographs of the selected area. Double-labeled neurons may appear as yellow. ***D–F***, Photomicrographs showing the co-localization between pSTAT5 and eGFP in GH-injected $SST^{\Delta GHR}$ mice. ***G–I***, Quantification indicating the percentage of ARH^{SST} (***G***), $BNST^{SST}$ (***H***), and CEA^{SST} (***I***) neurons that are responsive to GH (express pSTAT5). ***J–L***, Quantification indicating the number of ARH^{SST} (***J***), $BNST^{SST}$ (***K***), and CEA^{SST} (***L***) neurons. 3V, third ventricle; ARH, arcuate nucleus of the hypothalamus; BNST, bed nucleus of the stria terminalis; CEA, central nucleus of the amygdala. Scale bar = 100 μm. *$p < 0.05$, **$p < 0.01$, ****$p < 0.0001$ significant difference between groups (two-way ANOVA followed by Holm–Sidak's multiple comparisons test).

neurons may mediate GH's metabolic effects. To test this possibility, the metabolism of control and $SST^{\Delta GHR}$ mice were detailed assessed. No differences between control and $SST^{\Delta GHR}$ mice were observed in the body weight, fat mass, lean body mass, food intake, VO_2, respiratory quotient, and ambulatory activity, either in males (Fig. 3*A–I*) or females (Fig. 3*J–R*). Glucose tolerance (Fig. 4*A*,*B*), insulin sensitivity (Fig. 4*C*,*D*), and counter-regulatory response to 2DG (Fig. 4*E*,*F*) did not differ between control and $SST^{\Delta GHR}$ mice. Thus, despite the numerous SST neurons that are responsive to GH, GHR ablation in these cells does not affect energy and glucose metabolism.

GH action in SST neurons regulates anxiety in a sex-dependent manner

Possible changes in anxiety were determined in $SST^{\Delta GHR}$ mice, compared to control animals. Using the open-field test, we observed a tendency ($t_{(23)} = 1.91$, $p = 0.06$) of the $SST^{\Delta GHR}$ male mice to spend less time in the center of the arena (Fig. 5*A*), suggesting increased anxiety-like behavior. However, no difference in the time spent in the center of the open field was observed between control and $SST^{\Delta GHR}$ female mice (Fig. 5*B*). Number of entries in the center and total distance traveled as well as duration and frequency of grooming, walking, rearing, sniffing, and stationary state were also analyzed in the open field, but no significant differences were observed between the groups either in males or females (Table 2). Anxiety was further evaluated by measuring the number of transitions across the different compartments in the light-dark box test (Crawley and Goodwin, 1980). Confirming the previous results obtained in the open-field test, $SST^{\Delta GHR}$ male mice showed a reduced number of transitions in the light-dark box test compared to control animals (Fig. 5*C*), whereas $SST^{\Delta GHR}$ female mice presented similar anxiety-like behavior compared to control females (Fig. 5*D*). No differences

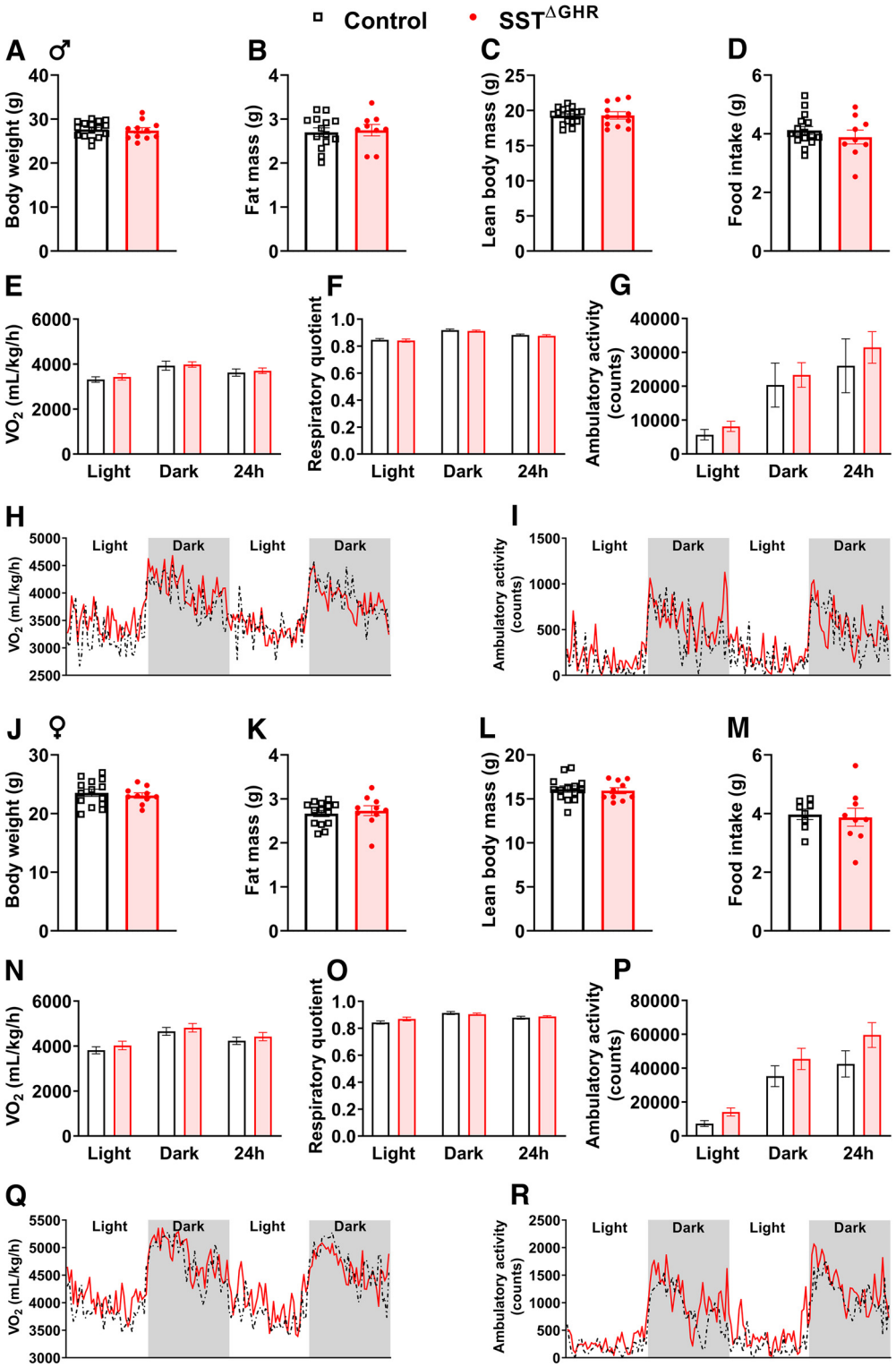

Figure 3. GHR ablation in SST neurons does not affect energy homeostasis. ***A–D***, Body weight, fat mass, lean body mass, and daily food intake of control ($n = 14$–16) and $SST^{\Delta GHR}$ ($n = 9$–11) male mice. ***E–I***, Oxygen consumption (VO_2), respiratory quotient (VCO_2/VO_2), and ambulatory activity of control ($n = 5$) and $SST^{\Delta GHR}$ ($n = 9$) male mice. ***J–M***, Body weight, fat mass, lean body mass, and daily food intake of control ($n = 8$–14) and $SST^{\Delta GHR}$ ($n = 9$–10) female mice. ***N–R***, VO_2, respiratory quotient, and ambulatory activity of control ($n = 7$) and $SST^{\Delta GHR}$ ($n = 8$) female mice. Possible differences between groups were analyzed by *t* test.

between groups were observed in the time spent and the distance traveled in the light zone during the light-dark box test (Table 2). Next, the elevated plus maze test was also employed to measure anxiety. The total distance traveled during the elevated plus maze test was similar between control and $SST^{\Delta GHR}$ mice, either in males (Fig. 5*E*) or females (Fig. 5*I*). However, $SST^{\Delta GHR}$ male mice showed a decrease in the time spent in the open arms (Fig. 5*F*), in the time moving in the open arms (Fig. 5*G*), and in the distance traveled in the open arms (Fig. 5*H*), when compared to control animals. $SST^{\Delta GHR}$ female mice exhibited normal behavior in the

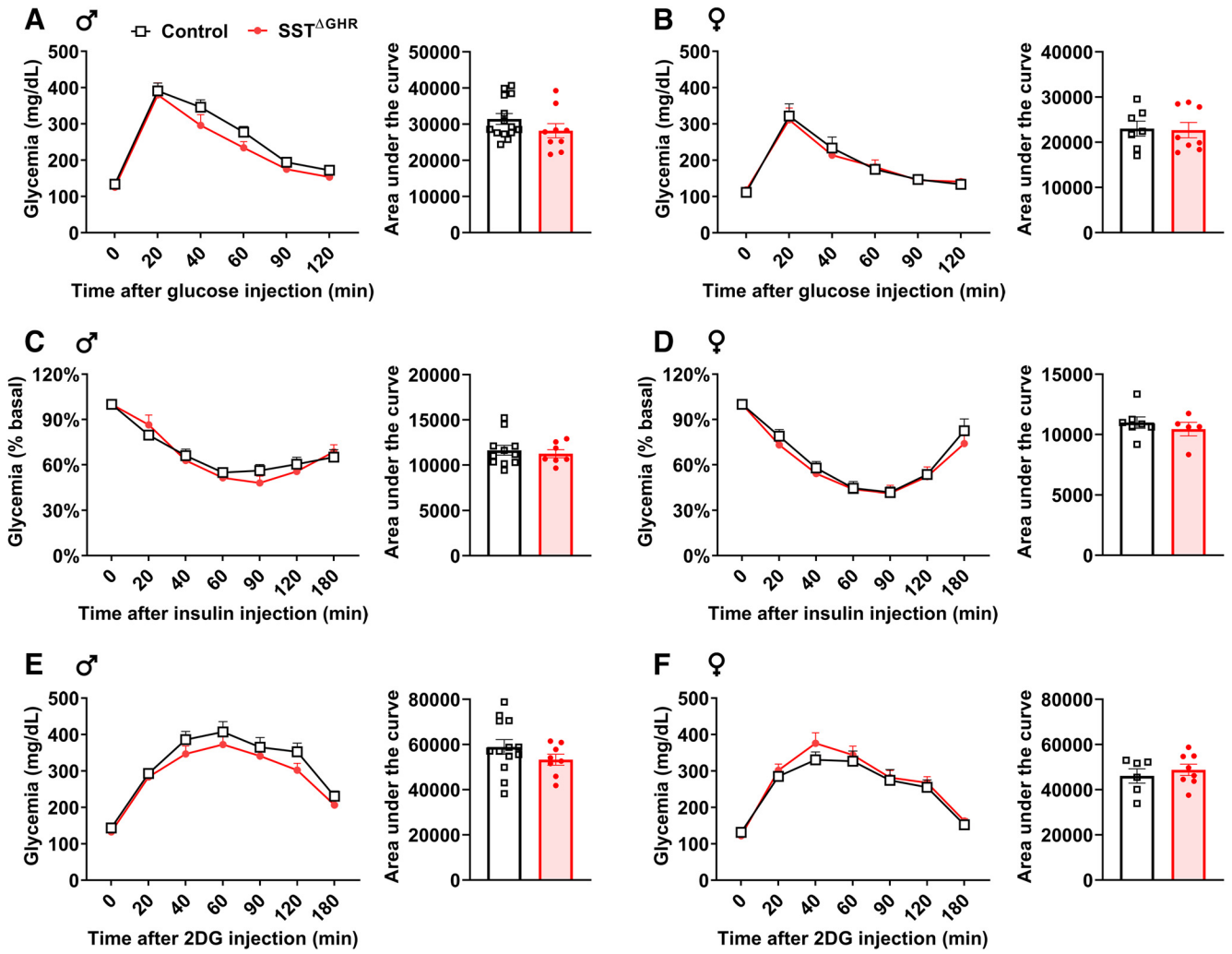

Figure 4. GHR ablation in SST neurons does not affect glucose homeostasis. ***A–F***, Blood glucose levels and area under the curve of the glucose tolerance test, insulin tolerance test, and counter-regulatory response to 2-deoxy-D-glucose (2DG) in control males ($n = 11–14$), $SST^{\Delta GHR}$ males ($n = 7–9$), control females ($n = 6–7$) and $SST^{\Delta GHR}$ females ($n = 5–8$). Possible differences between groups in the areas under the curve were analyzed by *t* test.

elevated plus maze test (Fig. 5*J–L*). Taken together, distinct behavioral tests indicate that GHR ablation in SST neurons increases anxiety-like behavior in male mice, but not in females.

GHR ablation in SST-expressing neurons decreases fear response in male and female mice

In this experiment, mice were exposed to auditory Pavlovian fear conditioning. Control and $SST^{\Delta GHR}$ mice exhibited similar fear acquisition in both sexes (Fig. 6*A*,*D*). Notably, when the fear of the tone was later tested in a novel context, $SST^{\Delta GHR}$ mice exhibited a significant reduction in fear response, which was determined by the time the animal spends in freezing. Differently from what had been observed in the evaluation of anxiety, the fear response was reduced in both male (Fig. 6*B*,*C*) and female (Fig. 6*E*,*F*) $SST^{\Delta GHR}$ mice. To determine whether $SST^{\Delta GHR}$ mice have defects in any type of memory or specifically regarding fear memory, the novel object recognition test was used. Control and $SST^{\Delta GHR}$ mice explored each object approximately 50% of the time during the training period, indicating no preference for any object (Fig. 7*A*,*C*). On the test day (24 h later), mice explored significantly more the new object, in comparison with the old one, without differences between male and female control and $SST^{\Delta GHR}$ mice (Fig. 7*B*,*D*). Thus, GHR ablation in SST-expressing neurons decreases fear memory in both male and female mice but does not affect recognition memory.

Transcripts associated with synaptic plasticity and function are differently expressed in the amygdala of $SST^{\Delta GHR}$ mice with marked differences between males and females

The amygdala plays a fundamental role in the regulation of neuropsychiatric diseases, such as depression, anxiety, and posttraumatic stress disorder (Shackman and Fox, 2016). Furthermore, previous studies have suggested that GH action in the amygdala regulates fear memory (Meyer et al., 2014; Gisabella et al., 2016). Here, we showed that a high percentage of CEA^{SST} neurons are responsive to GH (Fig. 2*C*). Thus, we decided to analyze the gene expression in the amygdala through a bilateral punch comprising the CEA and BLA. In male mice, a 20% reduction in the *Ghr* mRNA levels was observed in the amygdala of $SST^{\Delta GHR}$ mice, compared to control animals (Fig. 8). This finding further confirms the *Ghr* inactivation in a subset of amygdala (SST-expressing) neurons. *Sst* mRNA levels were reduced by 50% in $SST^{\Delta GHR}$ mice, whereas no changes in *Crh*, *Gh*, and *Ghsr* (ghrelin receptor) expression were observed between groups (Fig. 8). Different subunits of the glutamate receptors (*Gria1*, *Grin1*, *Grin2a*, and *Grin2b*), GABA receptors (*Gabra1* and *Gabbr1*), potassium

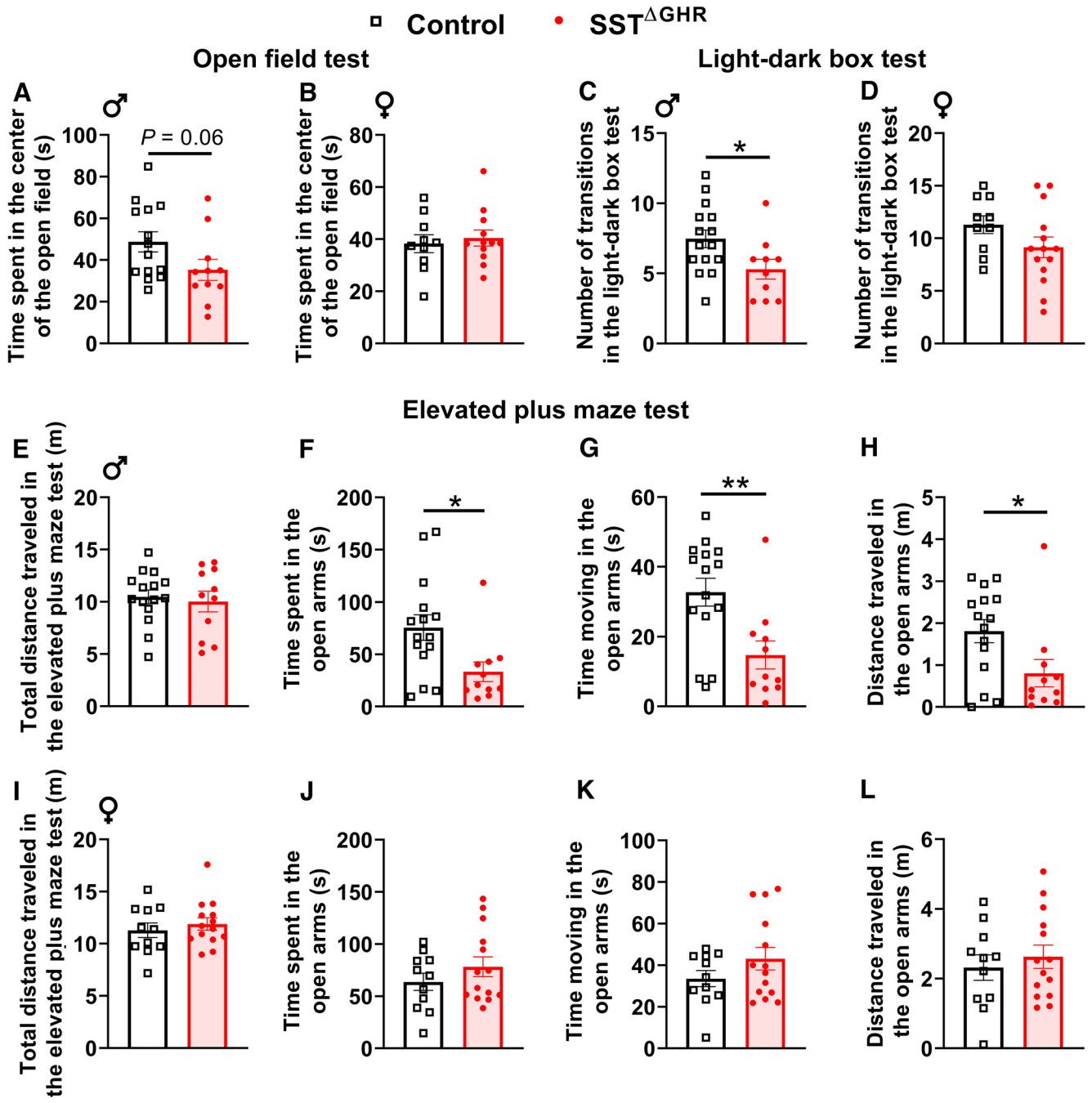

Figure 5. GH action in SST neurons regulates anxiety in a sex-dependent manner. ***A–D***, Time spent in the center of the open field and number of transitions in the light-dark box test in control males ($n = 14$–15), $SST^{\Delta GHR}$ males ($n = 10$–11), control females ($n = 10$) and $SST^{\Delta GHR}$ females ($n = 12$–14). ***E–L***, Total distance traveled in the elevated plus maze test, time spent in the open arms, time moving in the open arms and distance traveled in the open arms in control males ($n = 15$), $SST^{\Delta GHR}$ males ($n = 11$), control females ($n = 11$) and $SST^{\Delta GHR}$ females ($n = 14$). *$p < 0.05$, **$p < 0.01$ significant difference between groups (*t* test).

channels (*Kcnj8* and *Kcnj11*), dopamine receptors (*Dr2d*), and genes related to memory and synaptic neurotransmission and plasticity (*Slc32a1*, *Creb1*, *Dlg4*, and *Nrg1*) were analyzed, but no differences between control and $SST^{\Delta GHR}$ mice were found (Fig. 8). However, a significant increase in the mRNA expression of *Gabbr2* (encodes the $GABA_{B2}$ receptor), *Syp* (encodes the synaptophysin), and *Bdnf* (encodes the brain-derived neurotrophic factor) was observed in the amygdala of $SST^{\Delta GHR}$ mice, compared to control animals (Fig. 8). *Slc17a7* mRNA levels (encodes the vesicular glutamate transporter 1) tended to be increased ($t_{(19)} = 2.01$, $p = 0.059$) in the amygdala of $SST^{\Delta GHR}$ mice, when compared to control animals (Fig. 8). In female mice, *Ghr* and *Sst* mRNA levels were also reduced in the amygdala of $SST^{\Delta GHR}$ mice, compared to control animals (Fig. 8). However, differently than the findings observed in males, $SST^{\Delta GHR}$ female mice presented a reduction in *Grin1* (encodes a subunit of the glutamate NMDA receptor), *Slc17a7*, and *Dlg4* mRNA expression, whereas *Gabra1* (encodes the $GABA_A$ receptor) and *Gabbr1* (encodes the $GABA_{B1}$ receptor) mRNA levels were increased, compared to control females (Fig. 8). Thus, GHR ablation in SST neurons caused sex-dependent changes in the amygdalar expression of factors involved in synaptic plasticity and function.

Table 2. Additional behavioral states

	Males		Females	
Behavior	Control	$SST^{\Delta GHR}$	Control	$SST^{\Delta GHR}$
Open field test				
Entries in the center	28.8 ± 2.4	25.5 ± 2.2	34.0 ± 3.3	33.0 ± 2.2
Total distance traveled (m)	15.1 ± 1.2	14.7 ± 1.2	14.7 ± 1.2	19.9 ± 1.5
Grooming (duration*)	15.0 ± 2.4	17.4 ± 1.5	10.6 ± 1.6	9.1 ± 1.3
Grooming (# of bouts)	9.5 ± 1.3	10.1 ± 1.1	6.9 ± 0.8	6.4 ± 0.7
Walking (duration)	232.5 ± 8.9	215.8 ± 8.4	237.8 ± 8.6	256.6 ± 6.4
Walking (# of bouts)	15.7 ± 1.1	18.6 ± 1.2	15.3 ± 1.8	12.0 ± 1.1
Rearing (duration)	34.5 ± 3.3	26.3 ± 2.5	23.7 ± 2.4	30.4 ± 3.9
Rearing (# of bouts)	70.3 ± 5.5	59.6 ± 3.8	27.4 ± 2.6	33.6 ± 3.5
Sniffing (duration)	61.8 ± 5.3	50.1 ± 5.0	51.9 ± 3.1	55.7 ± 4.0
Sniffing (# of bouts)	154.3 ± 8.6	152.3 ± 5.6	139.5 ± 6.9	145.4 ± 7.4
Stationary (duration)	67.5 ± 8.9	84.2 ± 8.4	62.2 ± 8.6	43.4 ± 6.4
Stationary (# of bouts)	15.1 ± 1.1	18.1 ± 1.3	14.6 ± 1.8	11.2 ± 1.2
Light-dark box test				
Time spent in the light zone (s)	97.5 ± 9.3	92.7 ± 14.1	112.1 ± 7.7	103.3 ± 8.4
Distance traveled in the light zone (m)	4.5 ± 0.4	4.7 ± 0.7	6.2 ± 0.5	6.2 ± 0.5

*Duration is expressed in seconds. Data are shown as mean ± SEM. Possible differences between control and $SST^{\Delta GHR}$ mice in each sex were analyzed by *t* test.

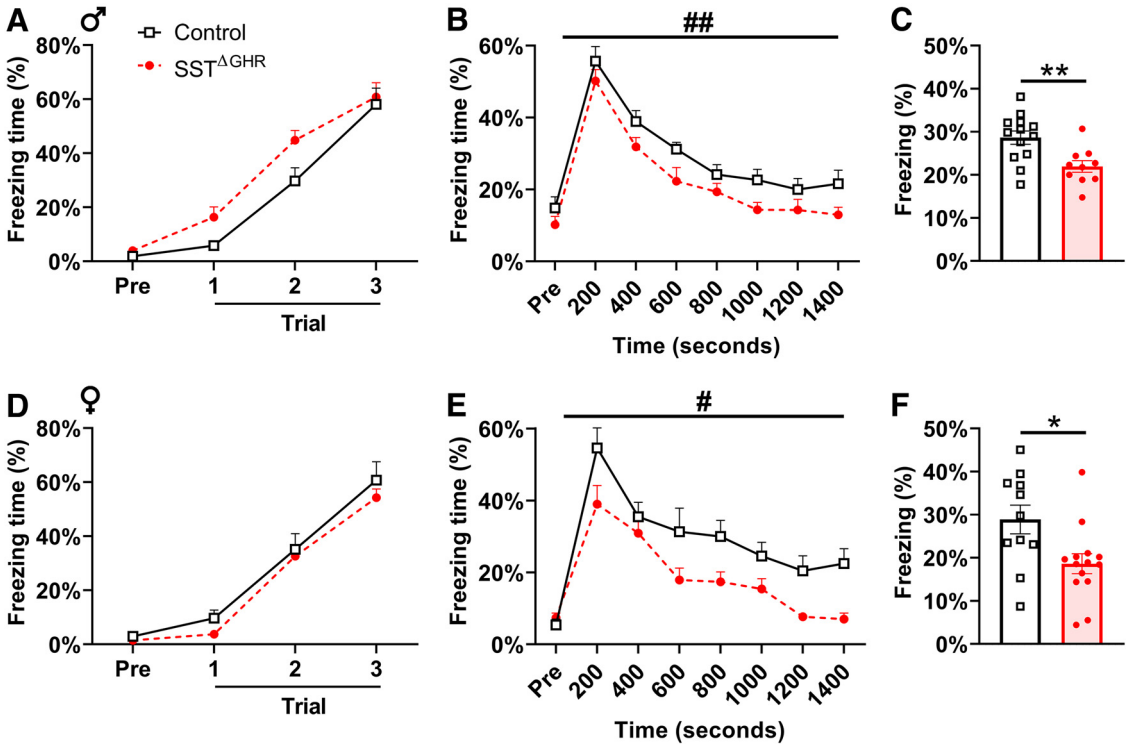

Figure 6. GHR ablation in SST-expressing neurons decreases fear response in male and female mice. ***A***, Percentage of time in freezing demonstrating the fear acquisition of male mice during the auditory Pavlovian fear conditioning. ***B***, ***C***, Fear response to sequential tones (40 conditioned stimulus presentations with a duration of 30 s each and 5-s intervals between them) evaluated 24 h after the fear conditioning in control ($n = 13$) and $SST^{\Delta GHR}$ ($n = 10$) male mice. The percentage of time in freezing was displayed in 200-s intervals and the mean percentage in freezing was calculated for each animal. ***D***, Percentage of time in freezing demonstrating the fear acquisition of female mice during the auditory Pavlovian fear conditioning. ***E***, ***F***, Fear response to sequential tones evaluated 24 h after the fear conditioning in control ($n = 11$) and $SST^{\Delta GHR}$ ($n = 14$) female mice. #$p < 0.05$, ##$p < 0.01$ main effect of GHR ablation (repeated measures two-way ANOVA). *$p < 0.05$, **$p < 0.01$ significant difference between groups (*t* test).

ERα is expressed in a small group of ARH^{SST} neurons

ERα is expressed in different hypothalamic areas and subnuclei of the amygdala (Simerly et al., 1990). Thus, to investigate whether SST neurons are sensitive to changes in estrogen levels, which could help to explain the sex differences observed in the present study, the percentages of ARH^{SST}, $BNST^{SST}$ and CEA^{SST} neurons that express ERα were determined in male and female mice. ERα expression was abundantly found in the ARH (Fig. 9*A*,*D*) and other areas, such as the ventrolateral part of the ventromedial nucleus of the hypothalamus and medial nucleus of the amygdala (data not shown). However, only approximately 7% of ARH^{SST} neurons expressed ERα in males and females (Fig. 9*G*,*H*). Few ERα positive cells were found in the BNST (Fig. 9*B*,*E*) and CEA (Fig. 9*C*,*F*) and virtually no $BNST^{SST}$ (dorsolateral subdivision) and CEA^{SST} neuron expressed ERα (Fig. 9*G*,*H*).

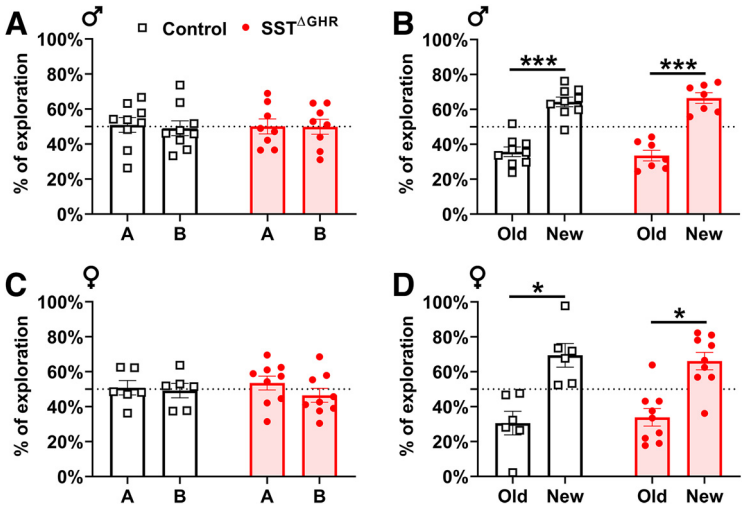

Figure 7. GHR ablation in SST neurons does not affect recognition memory. ***A***, Training session in the novel object recognition test showed that none of the objects used evoked innate preference in male mice. ***B***, Evaluation of the recognition memory (24 h after the training session) by replacing a familiar object (old) with a new one in control ($n = 9$) and $SST^{\Delta GHR}$ ($n = 7–8$) male mice. ***C***, Training session in the novel object recognition test showing that none of the objects used evoked innate preference in female mice. ***D***, Evaluation of the recognition memory (24 h after the training session) by replacing a familiar object (old) with a new one in control ($n = 6$) and $SST^{\Delta GHR}$ ($n = 9$) female mice. *$p < 0.05$, ***$p < 0.001$ significant difference between the old and new objects (repeated measures two-way ANOVA).

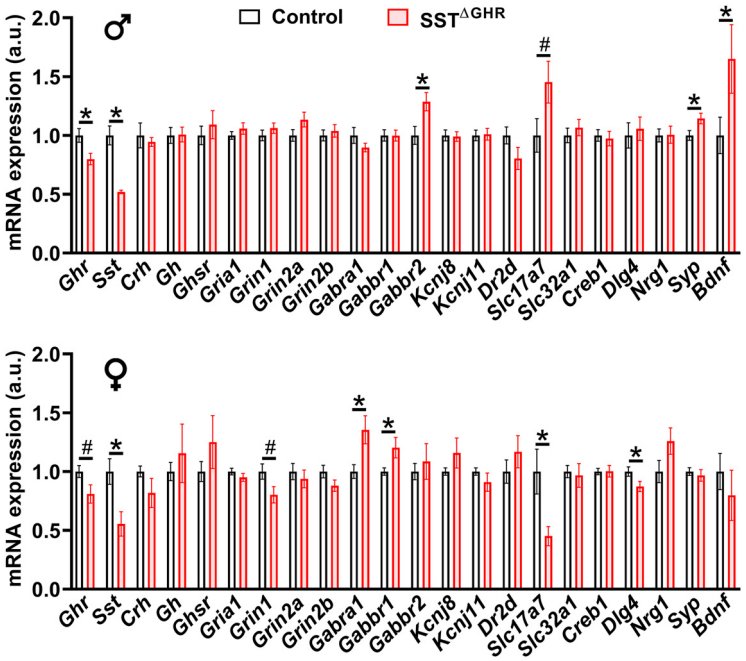

Figure 8. Gene expression analysis in a micro punch comprising the central nucleus of the amygdala and basolateral complex. mRNA levels (arbitrary units, a.u.) were determined in control ($n = 13$) and $SST^{\Delta GHR}$ ($n = 10$) male mice, and in control ($n = 9$) and $SST^{\Delta GHR}$ ($n = 9$) female mice. *$p < 0.05$ significant difference between groups (*t* test). #$p < 0.06$ (*t* test).

Discussion

In the current study, we observed that GHR ablation in SST-expressing cells led to increased anxiety-like behavior in male mice and reduced fear memory in both sexes. These findings are in accordance with studies indicating that GH deficiency increases anxiety (Karachaliou et al., 2021) and the blockade of GH action in the amygdala reduces fear memory (Meyer et al., 2014). The absence of memory deficit in the object recognition test indicates that $SST^{\Delta GHR}$ mice exhibit specific alterations in fear memory and not in other types of memory (e.g., recognition or novelty). Of note, mice carrying a neuronal-specific STAT5 ablation also exhibit a reduction in contextual fear memory (Furigo et al., 2018). Thus, GHR signaling likely relies on the transcription factor STAT5 to modulate fear memory. Therefore, disruption of GHR signaling in SST-expressing neurons affects behavioral aspects associated with neuropsychiatric disorders.

A previous study already investigated the consequences on the somatotropic axis of GHR ablation in SST neurons. Unexpectedly, both male and female $SST^{\Delta GHR}$ mice show no significant alterations in pulsatile GH secretion, serum insulin-like growth factor-1 (IGF-1) levels, hepatic IGF-1 expression or body growth (Chaves et al., 2022). Thus, early-life GHR ablation in SST cells is insufficient to disturb the somatotropic axis and body growth, probably via compensatory mechanisms (e.g., negative

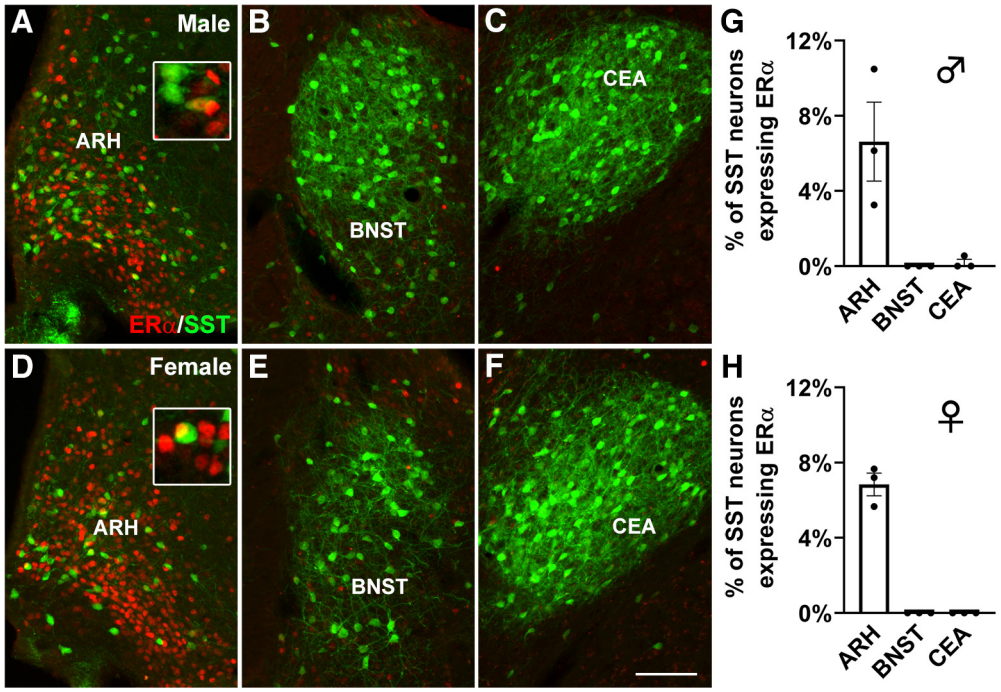

Figure 9. ERα is expressed only in a small group of ARH^{SST} neurons. ***A–F***, Epifluorescence photomicrographs showing the co-localization between ERα (red) and eGFP (green representing SST-expressing cells) in SST-eGFP reporter male and female mice. The insets represent higher magnification photomicrographs. ***G***, ***H***, Quantification indicating the percentage of ARH^{SST}, BNST^{SST} and CEA^{SST} neurons that express ERα. Scale bar = 100 μm. Two-way ANOVA was used for the comparison between male and female mice in the different areas analyzed.

feedback loop mediated by GH and IGF-1 in other hypothalamic neuronal populations or somatotrophs). In the present study, we confirmed that SST$^{\Delta GHR}$ mice exhibited normal body weight and composition, which is in accordance with the lack of changes in GH secretion.

It is known that central GH action regulates metabolism (Furigo et al., 2019b; Donato et al., 2021; Tavares et al., 2023), and SST-expressing cells control different metabolic aspects (Campbell et al., 2017; Zhu et al., 2017; Luo et al., 2018; Zséli et al., 2018; Stengel and Taché, 2019; Kumar and Singh, 2020; Suresh Nair et al., 2022). Our findings indicate that GHR signaling in SST-expressing cells is not involved in the regulation of energy and glucose homeostasis. Since metabolic alterations represent confounding factors that can affect behavior and neurological function, the absence of such changes in SST$^{\Delta GHR}$ mice further supports the direct role of GH action on SST neurons in controlling the predisposition to neuropsychiatric disorders. However, we only studied ad libitum fed mice consuming regular chow. So, we cannot rule out possible metabolic alterations of SST$^{\Delta GHR}$ mice under different metabolic conditions, such as calorie restriction or high-fat diet intake.

SST$^{\Delta GHR}$ male mice exhibited increased anxiety-like behavior in the light-dark box and elevated plus maze tests, and a tendency to expend less time in the center of the open field. The lack of statistical significance in the open field may be explained by the reduced sensitivity of this test to evaluate unconditioned anxiety in certain conditions (Ennaceur, 2014; Sturman et al., 2018). Nonetheless, we obtained robust evidence that GHR ablation in SST neurons increases anxiety in male mice. Noteworthy, the open field generally produces reliable results evaluating locomotor activity and exploratory behaviors. In this regard, we found no evidence that SST$^{\Delta GHR}$ mice present changes in locomotor activity during both the behavioral tests and the evaluation of metabolism.

The involvement of SST-expressing neurons in the regulation of anxiety is well-established (Engin et al., 2008; Engin and Treit, 2009; Wohleb et al., 2016; Fuchs et al., 2017; Pantazopoulos et al., 2017; Ahrens et al., 2018; Sun et al., 2020; Bruzsik et al., 2021; Xiao et al., 2021). For example, optogenetic activation of the CEA^{SST} projections to the central sublenticular extended amygdala causes an anxiogenic response without affecting locomotor activity (Sun et al., 2020). CEA^{SST} neurons are mostly GABAergic (Raver et al., 2020; Hogri et al., 2022) and another study showed that mice lacking the enzyme glutamate decarboxylase 67 in SST-expressing cells exhibit anxiety-like behavior, but no differences in locomotor activity (Miyata et al., 2019). The fact that GHR ablation in SST neurons led to alterations in anxiety only in male mice is not surprising because the pattern of GH secretion is sexually dimorphic (Steyn et al., 2016) and numerous studies have demonstrated marked sex differences in the role played by the extended amygdala, and in particular of SST neurons, in the control of anxiety and other behaviors (Dao et al., 2020; Diab et al., 2020; Jefferson et al., 2020; Englund et al., 2021; Kirson et al., 2021; Urien et al., 2021; Suresh Nair et al., 2022; Urien and Bauer, 2022). Accordingly, alterations in the activity of CEA^{SST} neurons by early life stress induce anxiety-like behavior in males but not female rodents (Englund et al., 2021). Female rats on proestrus, which is a phase of the estrous cycle characterized by high levels of estrogen, exhibit greater anxiolytic effects of diazepam (Ravenelle et al., 2018). Thus, sex differences in anxiety-like behavior are likely modulated by sex hormone receptors (Borrow and Handa, 2017). However, since BNST^{SST} and CEA^{SST} neurons do not express ERα, estrogens act in other neuronal populations to modulate mood. Of note, the estrous cycle of the females was not determined in our study, which could have increased the variability in the evaluated responses.

Although the pituitary gland is responsible for secreting GH into the systemic circulation (Steyn et al., 2016), chronic stress enhances GH expression in the BLA (Meyer et al., 2014). Virus-

mediated GH overexpression in the BLA enhances long-term fear memory, whereas GHR signaling blockade in the amygdala prevents ghrelin-induced increases in fear response (Meyer et al., 2014). Whether amygdala-derived GH presents a local or endocrine function is currently unknown. However, the present and previous studies (Furigo et al., 2017; Wasinski et al., 2021a) indicate that a systemic or central GH stimulus induces pSTAT5 immunoreactive cells only in the CEA, whereas BLA exhibits a small number of GH-responsive cells. Thus, a paracrine communication possibly exists between BLA and CEA. So, GH produced in BLA cells may act on GHR-expressing neurons of the CEA. Although it was not our scope to precisely identify the subgroup of SST neurons involved in this response, previous studies provided robust evidence that GHR signaling in the amygdala regulates fear memory (Meyer et al., 2014; Gisabella et al., 2016). Thus, GH's effects on fear memory are likely mediated by CEA^{SST} neurons, although the participation of other neuronal populations, such as $BNST^{SST}$ and ARH^{SST}, is also possible. Thus, a limitation of our study was our incapacity in determining the specific nucleus involved in the behavioral phenotype of $SST^{\Delta GHR}$ mice. On the other hand, our study highlighted the great importance of GHR^{SST} neurons in controlling anxiety and fear memory.

CEA and BLA were collected to analyze possible changes in gene expression. The 20% reduction in the amygdalar *Ghr* expression is in accordance with the genetic ablation only in SST-expressing and the maintenance of this receptor in other cell types present in the CEA. SST^{Cre} mouse model exhibits reduced SST expression, explaining our gene expression result (Viollet et al., 2017). However, even in homozygosity when SST expression is much lower compared to heterozygous animals (as in our study), SST^{Cre} mice do not exhibit significant behavioral alterations, including tests that evaluated anxiety-like and depression-like symptoms (Viollet et al., 2017). GH administration regulates synaptic plasticity, and excitatory and inhibitory synaptic transmission (Olivares-Hernández et al., 2018; G.Y. Li et al., 2023), including in the amygdala (Gisabella et al., 2016). GHR ablation in SST neurons led to changes in the mRNA expression of GABA and glutamate receptors, neurotropic factors and proteins associated with synaptic transmission in the amygdala. Although it is unclear how the changes in the expression of these transcripts could explain the behavioral phenotype of $SST^{\Delta GHR}$ mice, these findings suggest that alterations in GHR signaling is likely sufficient to cause a significant impact on synaptic plasticity and function in the amygdala. However, additional studies are necessary to establish a causal relationship between the alterations in the expression of these genes and the behavioral changes observed in $SST^{\Delta GHR}$ mice. Furthermore, the striking differences observed between male and female $SST^{\Delta GHR}$ mice on changes in gene expression in the amygdala further supports a sex-dependent effect of GH action regulating behavior.

In conclusion, the present study identified the SST neurons as a key cell population responsible for mediating the effects of GH on neurological aspects associated with neuropsychiatric diseases. Thus, behavioral and mood problems caused by endocrine dysfunctions, such as GH deficiency or acromegaly, can be better understood. It is worth mentioning that aging is accompanied by a well-documented decrease in GH secretion. Therefore, future studies should investigate the potential association between GH, SST neurons, and neuropsychiatric disorders during aging. Finally, our study reiterates the importance of GH action in the brain to regulate important physiological functions.

References

Ahrens S, Wu MV, Furlan A, Hwang GR, Paik R, Li H, Penzo MA, Tollkuhn J, Li B (2018) A Central extended amygdala circuit that modulates anxiety. J Neurosci 38:5567–5583.

Besnard A, Gao Y, TaeWoo Kim M, Twarkowski H, Reed AK, Langberg T, Feng W, Xu X, Saur D, Zweifel LS, Davison I, Sahay A (2019) Dorsolateral septum somatostatin interneurons gate mobility to calibrate context-specific behavioral fear responses. Nat Neurosci 22:436–446.

Binder EB (2009) The role of FKBP5, a co-chaperone of the glucocorticoid receptor in the pathogenesis and therapy of affective and anxiety disorders. Psychoneuroendocrinology 34 [Suppl 1]:S186–S195.

Bohlooly-Y M, Olsson B, Bruder CE, Lindén D, Sjögren K, Bjursell M, Egecioglu E, Svensson L, Brodin P, Waterton JC, Isaksson OG, Sundler F, Ahrén B, Ohlsson C, Oscarsson J, Törnell J (2005) Growth hormone overexpression in the central nervous system results in hyperphagia-induced obesity associated with insulin resistance and dyslipidemia. Diabetes 54:51–62.

Borrow AP, Handa RJ (2017) Estrogen receptors modulation of anxiety-like behavior. Vitam Horm 103:27–52.

Bruzsik B, Biro L, Zelena D, Sipos E, Szebik H, Sarosdi KR, Horvath O, Farkas I, Csillag V, Finszter CK, Mikics E, Toth M (2021) Somatostatin neurons of the bed nucleus of stria terminalis enhance associative fear memory consolidation in mice. J Neurosci 41:1982–1995.

Campbell JN, Macosko EZ, Fenselau H, Pers TH, Lyubetskaya A, Tenen D, Goldman M, Verstegen AM, Resch JM, McCarroll SA, Rosen ED, Lowell BB, Tsai LT (2017) A molecular census of arcuate hypothalamus and median eminence cell types. Nat Neurosci 20:484–496.

Chaves FM, Wasinski F, Tavares MR, Mansano NS, Frazao R, Gusmao DO, Quaresma PGF, Pedroso JAB, Elias CF, List EO, Kopchick JJ, Szawka RE, Donato J (2022) Effects of the isolated and combined ablation of growth hormone and IGF-1 receptors in somatostatin neurons. Endocrinology 163:bqac045.

Chiba S, Numakawa T, Ninomiya M, Richards MC, Wakabayashi C, Kunugi H (2012) Chronic restraint stress causes anxiety- and depression-like behaviors, downregulates glucocorticoid receptor expression, and attenuates glutamate release induced by brain-derived neurotrophic factor in the prefrontal cortex. Prog Neuropsychopharmacol Biol Psychiatry 39:112–119.

Claes S (2009) Glucocorticoid receptor polymorphisms in major depression. Ann N Y Acad Sci 1179:216–228.

Crawley J, Goodwin FK (1980) Preliminary report of a simple animal behavior model for the anxiolytic effects of benzodiazepines. Pharmacol Biochem Behav 13:167–170.

Dao NC, Suresh Nair M, Magee SN, Moyer JB, Sendao V, Brockway DF, Crowley NA (2020) Forced abstinence from alcohol induces sex-specific depression-like behavioral and neural adaptations in somatostatin neurons in cortical and amygdalar regions. Front Behav Neurosci 14:86.

Deepak D, Daousi C, Boyland E, Pinkney JH, Wilding JP, MacFarlane IA (2008) Growth hormone and changes in energy balance in growth hormone deficient adults. Eur J Clin Invest 38:622–627.

Diab A, Qi J, Shahin I, Milligan C, Fawcett JP (2020) NCK1 regulates amygdala activity to control context-dependent stress responses and anxiety in male mice. Neuroscience 448:107–125.

Donato J Jr, Wasinski F, Furigo IC, Metzger M, Frazão R (2021) Central regulation of metabolism by growth hormone. Cells 10:129.

Dos Santos WO, Gusmao DO, Wasinski F, List EO, Kopchick JJ, Donato J Jr (2021) Effects of growth hormone receptor ablation in corticotropin-releasing hormone cells. Int J Mol Sci 22:9908.

Egecioglu E, Bjursell M, Ljungberg A, Dickson SL, Kopchick JJ, Bergström G, Svensson L, Oscarsson J, Törnell J, Bohlooly-Y M (2006) Growth hormone receptor deficiency results in blunted ghrelin feeding response, obesity, and hypolipidemia in mice. Am J Physiol Endocrinol Metab 290: E317–F325.

Engin E, Treit D (2009) Anxiolytic and antidepressant actions of somatostatin: the role of sst2 and sst3 receptors. Psychopharmacology 206:281–289.

Engin E, Stellbrink J, Treit D, Dickson CT (2008) Anxiolytic and antidepressant effects of intracerebroventricularly administered somatostatin: behavioral and neurophysiological evidence. Neuroscience 157:666–676.

Englund J, Haikonen J, Shteinikov V, Amarilla SP, Atanasova T, Shintyapina A, Ryazantseva M, Partanen J, Voikar V, Lauri SE (2021) Downregulation of kainate receptors regulating GABAergic transmission in amygdala after

early life stress is associated with anxiety-like behavior in rodents. Transl Psychiatry 11:538.
Ennaceur A (2014) Tests of unconditioned anxiety - pitfalls and disappointments. Physiol Behav 135:55–71.
Fuchs T, Jefferson SJ, Hooper A, Yee PH, Maguire J, Luscher B (2017) Disinhibition of somatostatin-positive GABAergic interneurons results in an anxiolytic and antidepressant-like brain state. Mol Psychiatry 22:920–930.
Furigo IC, Metzger M, Teixeira PD, Soares CR, Donato J Jr (2017) Distribution of growth hormone-responsive cells in the mouse brain. Brain Struct Funct 222:341–363.
Furigo IC, Melo HM, Lyra E Silva NM, Ramos-Lobo AM, Teixeira PDS, Buonfiglio DC, Wasinski F, Lima ER, Higuti E, Peroni CN, Bartolini P, Soares CRJ, Metzger M, de Felice FG, Donato J, Jr. (2018) Brain STAT5 signaling modulates learning and memory formation. Brain Struct Funct 223:2229–2241.
Furigo IC, de Souza GO, Teixeira PDS, Guadagnini D, Frazão R, List EO, Kopchick JJ, Prada PO, Donato J Jr (2019a) Growth hormone enhances the recovery of hypoglycemia via ventromedial hypothalamic neurons. FASEB J 33:11909–11924.
Furigo IC, Teixeira PDS, de Souza GO, Couto GCL, Romero GG, Perelló M, Frazão R, Elias LL, Metzger M, List EO, Kopchick JJ, Donato J Jr (2019b) Growth hormone regulates neuroendocrine responses to weight loss via AgRP neurons. Nat Commun 10:662.
Gisabella B, Farah S, Peng X, Burgos-Robles A, Lim SH, Goosens KA (2016) Growth hormone biases amygdala network activation after fear learning. Transl Psychiatry 6:e960.
Gupta D, Patterson AM, Osborne-Lawrence S, Bookout AL, Varshney S, Shankar K, Singh O, Metzger NP, Richard CP, Wyler SC, Elmquist JK, Zigman JM (2021) Disrupting the ghrelin-growth hormone axis limits ghrelin's orexigenic but not glucoregulatory actions. Mol Metab 53:101258.
Hogri R, Teuchmann HL, Heinke B, Holzinger R, Trofimova L, Sandkuhler J (2022) GABAergic CaMKIIα+ amygdala output attenuates pain and modulates emotional-motivational behavior via parabrachial inhibition. J Neurosci 42:5373–5388.
Jefferson SJ, Feng M, Chon U, Guo Y, Kim Y, Luscher B (2020) Disinhibition of somatostatin interneurons confers resilience to stress in male but not female mice. Neurobiol Stress 13:100238.
Karachaliou FH, Karavanaki K, Simatou A, Tsintzou E, Skarakis NS, Kanaka-Gatenbein C (2021) Association of growth hormone deficiency (GHD) with anxiety and depression: experimental data and evidence from GHD children and adolescents. Hormones (Athens) 20:679–689.
Kim JH, Leggatt RA, Chan M, Volkoff H, Devlin RH (2015) Effects of chronic growth hormone overexpression on appetite-regulating brain gene expression in coho salmon. Mol Cell Endocrinol 413:178–188.
Kirson D, Khom S, Rodriguez L, Wolfe SA, Varodayan FP, Gandhi PJ, Patel RR, Vlkolinsky R, Bajo M, Roberto M (2021) Sex differences in acute alcohol sensitivity of naïve and alcohol dependent central amygdala GABA synapses. Alcohol Alcohol 56:581–588.
Kumar U, Singh S (2020) Role of somatostatin in the regulation of central and peripheral factors of satiety and obesity. Int J Mol Sci 21:2568.
Li GY, Wu QZ, Song TJ, Zhen XC, Yu X (2023) Dynamic regulation of excitatory and inhibitory synaptic transmission by growth hormone in the developing mouse brain. Acta Pharmacol Sin 44:1109–1121.
Li H, Penzo MA, Taniguchi H, Kopec CD, Huang ZJ, Li B (2013) Experience-dependent modification of a central amygdala fear circuit. Nat Neurosci 16:332–339.
List EO, Berryman DE, Funk K, Gosney ES, Jara A, Kelder B, Wang X, Kutz L, Troike K, Lozier N, Mikula V, Lubbers ER, Zhang H, Vesel C, Junnila RK, Frank SJ, Masternak MM, Bartke A, Kopchick JJ (2013) The role of GH in adipose tissue: lessons from adipose-specific GH receptor gene-disrupted mice. Mol Endocrinol 27:524–535.
Luo SX, Huang J, Li Q, Mohammad H, Lee CY, Krishna K, Kok AM, Tan YL, Lim JY, Li H, Yeow LY, Sun J, He M, Grandjean J, Sajikumar S, Han W, Fu Y (2018) Regulation of feeding by somatostatin neurons in the tuberal nucleus. Science 361:76–81.
Meyer RM, Burgos-Robles A, Liu E, Correia SS, Goosens KA (2014) A ghrelin-growth hormone axis drives stress-induced vulnerability to enhanced fear. Mol Psychiatry 19:1284–1294.
Miyata S, Kumagaya R, Kakizaki T, Fujihara K, Wakamatsu K, Yanagawa Y (2019) Loss of glutamate decarboxylase 67 in somatostatin-expressing neurons leads to anxiety-like behavior and alteration in the Akt/GSK3β signaling pathway. Front Behav Neurosci 13:131.
Nyberg F (2000) Growth hormone in the brain: characteristics of specific brain targets for the hormone and their functional significance. Front Neuroendocrinol 21:330–348.
Olivares-Hernández JD, García-García F, Camacho-Abrego I, Flores G, Juárez-Aguilar E (2018) Intracerebroventricular administration of growth hormone induces morphological changes in pyramidal neurons of the hippocampus and prefrontal cortex in adult rats. Synapse 72:e22030.
Pantazopoulos H, Wiseman JT, Markota M, Ehrenfeld L, Berretta S (2017) Decreased numbers of somatostatin-expressing neurons in the amygdala of subjects with bipolar disorder or schizophrenia: relationship to circadian rhythms. Biol Psychiatry 81:536–547.
Penzo MA, Robert V, Tucciarone J, De Bundel D, Wang M, Van Aelst L, Darvas M, Parada LF, Palmiter RD, He M, Huang ZJ, Li B (2015) The paraventricular thalamus controls a central amygdala fear circuit. Nature 519:455–459.
Pomrenze MB, Tovar-Diaz J, Blasio A, Maiya R, Giovanetti SM, Lei K, Morikawa H, Hopf FW, Messing RO (2019) A corticotropin releasing factor network in the extended amygdala for anxiety. J Neurosci 39:1030–1043.
Quaresma PGF, Teixeira PDS, Furigo IC, Wasinski F, Couto GC, Frazão R, List EO, Kopchick JJ, Donato J Jr (2019) Growth hormone/STAT5 signaling in proopiomelanocortin neurons regulates glucoprivic hyperphagia. Mol Cell Endocrinol 498:110574.
Quaresma PGF, Dos Santos WO, Wasinski F, Metzger M, Donato J Jr (2021) Neurochemical phenotype of growth hormone-responsive cells in the mouse paraventricular nucleus of the hypothalamus. J Comp Neurol 529:1228–1239.
Ravenelle R, Berman AK, La J, Mason B, Asumadu E, Yelleswarapu C, Donaldson ST (2018) Sex matters: females in proestrus show greater diazepam anxiolysis and brain-derived neurotrophin factor- and parvalbumin-positive neurons than males. Eur J Neurosci 47:994–1002.
Raver C, Uddin O, Ji Y, Li Y, Cramer N, Jenne C, Morales M, Masri R, Keller A (2020) An Amygdalo-parabrachial pathway regulates pain perception and chronic pain. J Neurosci 40:3424–3442.
Shackman AJ, Fox AS (2016) Contributions of the central extended amygdala to fear and anxiety. J Neurosci 36:8050–8063.
Simerly RB, Chang C, Muramatsu M, Swanson LW (1990) Distribution of androgen and estrogen receptor mRNA-containing cells in the rat brain: an in situ hybridization study. J Comp Neurol 294:76–95.
Stengel A, Taché Y (2019) Central somatostatin signaling and regulation of food intake. Ann N Y Acad Sci 1455:98–104.
Steyn FJ, Tolle V, Chen C, Epelbaum J (2016) Neuroendocrine regulation of growth hormone secretion. Compr Physiol 6:687–735.
Stilgenbauer L, de Lima JBM, Debarba LK, Khan M, Koshko L, Kopchick JJ, Bartke A, Schneider A, Sadagurski M (2023) Growth hormone receptor (GHR) in AgRP neurons regulates thermogenesis in a sex-specific manner. Geroscience 45:1745–1759.
Sturman O, Germain PL, Bohacek J (2018) Exploratory rearing: a context- and stress-sensitive behavior recorded in the open-field test. Stress 21:443–452.
Sun Y, Qian L, Xu L, Hunt S, Sah P (2020) Somatostatin neurons in the central amygdala mediate anxiety by disinhibition of the central sublenticular extended amygdala. Mol Psychiatry 1–12.
Suresh Nair M, Dao NC, Lopez Melean D, Griffith KR, Starnes WD, Moyer JB, Sicher AR, Brockway DF, Meeks KD, Crowley NA (2022) Somatostatin neurons in the bed nucleus of the stria terminalis play a sex-dependent role in binge drinking. Brain Res Bull 186:38–46.
Tavares MR, Frazao R, Donato J (2023) Understanding the role of growth hormone in situations of metabolic stress. J Endocrinol 256:e220159.
Teixeira PDS, Couto GC, Furigo IC, List EO, Kopchick JJ, Donato J Jr (2019) Central growth hormone action regulates metabolism during pregnancy. Am J Physiol Endocrinol Metab 317:E925–E940.
Urien L, Bauer EP (2022) Sex differences in BNST and amygdala activation by contextual, cued, and unpredictable threats. eNeuro 9:ENEURO.0233-0221.2021.
Urien L, Stein N, Ryckman A, Bell L, Bauer EP (2021) Extended amygdala circuits are differentially activated by context fear conditioning in male and female rats. Neurobiol Learn Mem 180:107401.
Viollet C, Simon A, Tolle V, Labarthe A, Grouselle D, Loe-Mie Y, Simonneau M, Martel G, Epelbaum J (2017) Somatostatin-IRES-Cre

mice: between knockout and wild-type? Front Endocrinol (Lausanne) 8:131.
Walf AA, Frye CA (2010) Estradiol reduces anxiety- and depression-like behavior of aged female mice. Physiol Behav 99:169–174.
Walf AA, Paris JJ, Frye CA (2009) Chronic estradiol replacement to aged female rats reduces anxiety-like and depression-like behavior and enhances cognitive performance. Psychoneuroendocrinology 34:909–916.
Wasinski F, Klein MO, Bittencourt JC, Metzger M, Donato J Jr (2021a) Distribution of growth hormone-responsive cells in the brain of rats and mice. Brain Res 1751:147189.
Wasinski F, Barrile F, Pedroso JAB, Quaresma PGF, Dos Santos WO, List EO, Kopchick JJ, Perelló M, Donato J (2021b) Ghrelin-induced food intake, but not GH secretion, requires the expression of the GH receptor in the brain of male mice. Endocrinology 162:bqab097.
Wohleb ES, Wu M, Gerhard DM, Taylor SR, Picciotto MR, Alreja M, Duman RS (2016) GABA interneurons mediate the rapid antidepressant-like effects of scopolamine. J Clin Invest 126:2482–2494.
Xiao Q, Zhou X, Wei P, Xie L, Han Y, Wang J, Cai A, Xu F, Tu J, Wang L (2021) A new GABAergic somatostatin projection from the BNST onto accumbal parvalbumin neurons controls anxiety. Mol Psychiatry 26:4719–4741.
Ye J, Veinante P (2019) Cell-type specific parallel circuits in the bed nucleus of the stria terminalis and the central nucleus of the amygdala of the mouse. Brain Struct Funct 224:1067–1095.
Zeidan MA, Igoe SA, Linnman C, Vitalo A, Levine JB, Klibanski A, Goldstein JM, Milad MR (2011) Estradiol modulates medial prefrontal cortex and amygdala activity during fear extinction in women and female rats. Biol Psychiatry 70:920–927.
Zhong C, Song Y, Wang Y, Zhang T, Duan M, Li Y, Liao L, Zhu Z, Hu W (2013) Increased food intake in growth hormone-transgenic common carp (*Cyprinus carpio* L.) may be mediated by upregulating agouti-related protein (AgRP). Gen Comp Endocrinol 192:81–88.
Zhu C, Yao Y, Xiong Y, Cheng M, Chen J, Zhao R, Liao F, Shi R, Song S (2017) Somatostatin neurons in the basal forebrain promote high-calorie food intake. Cell Rep 20:112–123.
Zséli G, Vida B, Szilvásy-Szabó A, Tóth M, Lechan RM, Fekete C (2018) Neuronal connections of the central amygdalar nucleus with refeeding-activated brain areas in rats. Brain Struct Funct 223:391–414.